How humidity can diminish avalanche risks: effect of grains properties (size, material)

Luc Oger, Claude El Tannoury, Renaud Delannay, Yves Le Gonidec, Irene Ippolito, Yanina Lucrecia Roht, Iñaki Gómez-Arriaran

How humidity can diminish avalanche risks: effect of grains properties (size, material)

Luc Oger,* Claude el Tannoury,† and Renaud Delannay‡

Univ. Rennes, CNRS, IPR [(Institut de Physique de Rennes)]-UMR 6251, F-35000 Rennes, France

Yves le Gonidec§

Univ. Rennes, CNRS, Géosciences Rennes - UMR 6118, F-35000 Rennes, France

Irene Ippolito¶ and Yanina Lucrecia Roht**

Universidad de Buenos Aires, Facultad de Ingeniería, Grupo de Medios Porosos, Av. Paseo Colón 850, Buenos Aires Argentina

Iñaki Gómez-Arriaran††

Department of Thermal Engineering. University of the Basque Country - UPV/EHU, Spain

(Dated: June 27, 2018)

Abstract

Laboratory study of slope stability remains a challenge for modeling, understanding and predicting natural dangerous events such as avalanches and landslide. We model these phenomena by using well known monosize beads packings experiments. We study the behavior of sphere packings submitted to continuous slow tilting process inside a humidity controlled environment. This study is carried out by varying the relative humidity range between 40 % and 94 %. We used monodisperse spherical grains (glass beads of $0.2, 0.5$ and 0.75 mm diameter and polystyrene beads of 0.15 mm diameter). First, the packing is prepared inside a parallelepiped box with different height (fully or partially filled) in a reproducible manner, then continuously and slowly tilted; the lateral and surface displacements of the spheres according to the tilted angle are recorded. Depending on the initial height, bead diameter and humidity, few successive "precursors", then avalanches can occur inside this box or flowing outside it. These results confirm that the cohesive forces between grains have a large impact on the stability of the granular medium. The role of the exposure time to the high humidity rates is observed in order to check the humidity diffusion process and to reach the hygroscopic equilibrium in the packing before the first avalanche. The continuous tilting process avoids the observation of this effect between the next consecutive avalanches.

PACS numbers: 45.70.Ht, 61.43.Gt, 83.80.Fg

Keywords: Avalanches, precursors of avalanches, sphere packings, humidity rates

*Electronic address: luc.oger@univ-rennes1.fr

†Electronic address: Claude-el-tannoury@univ-rennes1.fr

‡Electronic address: Reanud.delannay@univ-rennes1.fr

§Electronic address: yves.legonidec@univ-rennes1.fr

¶Electronic address: iippoli@fi.uba.ar

**Electronic address: lucreroht@gmail.com

††Electronic address: gomez.arriaran@ehu.eus

I. INTRODUCTION

Organized granular materials displacements occur in a large range of applications like concrete, ceramic, pharmaceutical products, agricultural grains, soils, powder metallurgy, and so on... In these cases, a large amount of grains are stored, pilled or displaced by moving unstable assemblies of grains. On the other hand, we can also discover grain displacements in many natural events like debris flows, snow avalanches, ice floes, flying ashes. So understanding the mechanics of these granular structures and destabilizations is a great subject of interest for numerous industrial domains and also natural events such as geophysical hazards. Understanding the initiation of these events can be a great improvement to prevent or stop these critical situations.

To observe the so-called precursor apparition (consist of a large number of simultaneous moves of grains uniformly distributed over the surface of the packing), some experimental studies [1–4] of three-dimensional avalanche events are performed at a laboratory scale but mostly in a dry atmosphere. We want to extend these studies also under a wet controlled atmosphere especially to be more close to some countries behaviors such as Argentina where they have relative humidity up to 100 % during several weeks. Indeed, in presence of moisture, grain interaction forces become more cohesive and, by consequence, the strength of the contact between beads is altered. These behaviors are related to the appearance of capillary interaction which is due to the formation of liquid bridges between grains depending on the moisture content [5]. In section II, we recollect the different information available in the previous precursor-avalanche studies and also about humidity effects on grains packings. Then we present the reproducible technique used to build a good homogeneous packing (section III). In the section IV we describe the principal techniques used to perform extensive analysis of our experiments. Then, in section V, we measure the different local or global quantities linked to the structural evolution of the grains packings during the tilting process depending on the different experimental conditions (grain size or properties, box filling, and so on...). In section VII we observe the effect of the exposure time to the high humidity rates on the avalanche and precursor evolutions, the so-called "maximum stability time" or hygroscopic equilibrium time".

II. SOME KNOWLEDGES ON THE PRECURSORS AND AVALANCHES STUDIES AND HUMIDITY EFFECTS

By tilting a granular medium, the tangential component of its weight increases causing friction on its whole and leading a superficial layer to a metastable state. When the angle of its surface becomes greater than its maximum stability angle θ_A, called angle of maximum stability, the avalanche occurs. After the avalanche, the angle of the new arrangement of the granular packing decreases to the angle of repose θ_R. Pile stability is controlled by several factors: system size (height [3], length [6] width [7]), pile density or volume compaction [1, 3, 8] and also rotation regime [9].

The destabilization of a granular pile is characterized by the presence of grains rearrangements occurring at the surface of the pile. Bretz et al. [10] then Nerone et al. [4] were the first to reproduce and to film these events in a slowly inclined box. Bretz et al. [10] were interested in the presence of these events between two successive avalanches. They found that the grains reorganization distribution follows a power law in function of their size. But they didn't indicate the presence of any large event occurring between two successive avalanches. As Nerone et al. [4], they were interested in the presence of these rearrangements before the first avalanche. They showed that the destabilization of granular pile goes through two types of events before avalanche production: (I) a small rearrangements occurring at low tilting angles, with power law size distribution function followed by, (II) a large and deep grain rearrangement, called "Precursors" that appears before $\approx 15°$ of avalanche production at quasi periodically tilting angles, with a non power law size distribution function. Later, several studies [6, 11, 12] were oriented to the precursor avalanches identification. Lets go in more details in the analysis of the different criteria which control the precursors and the avalanche appearances.

A. Dry avalanches

At rest, granular packings can sustain normal loads and shear stresses (such as a jammed structure), but if a threshold shear stress is exceeded, part of the material starts to flow. The discrete nature of granular materials renders their behavior very complex. Due to some external forces evolutions, the macroscopic behavior of granular media is related to

the evolving geometry of their contact network and, more specifically, to the nature of the contacts themselves (frictional collisional, sliding, cohesive or not). So for free surface flows of granular packings under the action of gravity, the "jamming transition" above a critical shear stress is simply evidenced by the existence of the angle of maximum stability of a pile,θ_A, associated with internal friction [13]. After the flow starts, the angle of the pile relaxes towards the angle of repose, θ_R, smaller than θ_A. Similar observations were made for granular flows in a rotating drum as a function of the rotation rate [14]. Generally, experiments were performed at a low rotating regime defined as the rolling or cascading ones controlled through the Froude number "$0.05 < Fr < 0.4$ with $Fr = \sqrt{(\omega^2\, D)/(2\, g)}$ which represents the ratio of centrifugal to gravitational acceleration [15]. As already mentioned, the behavior of inclined 3D granular media show that parameters like humidity, system dimensions, friction between grains, bottom roughness, time between avalanches or packing fraction can influence the value of the maximum angle of stability of a packing [1, 3, 6–8]. For example, Aguirre et al [1] concluded that the number of grain layers can influence the stability of a packing up to about ten layers, while it becomes independent of it for larger numbers of layers. We will see our observation of it later on in this article. Recently, few studies were developed in order to observe these phenomena. Bretz et al. [10] used a digital imaging technique to analyze the avalanches occurring during the slow inclination of a box. These large slides were separated by a sequence of rearrangements of the surface grains which were recorded by a camera. By contrast, Nerone et al. [2, 16] showed that the size of rearrangements at the surface of the packing increases with the inclination angle for freshly prepared piles filling a box. A few degrees before the avalanche starts, quasi-periodical large events are observed. Zaitsev et al [17] reported recently that the same kind of events occur in the bulk of a slowly inclined granular packing. These internal events were evidenced through nonlinear acoustical measurements by recording the acoustical signal component which is due to the self-nonlinearity of the granular material. These events were interpreted as quasi-periodic transient reorganizations of the weak-contact subnetwork occurring in the bulk of the packings. We are also studying these behaviors in our experimental setup in Rennes [18]. Staron et al. [19] investigated the evolution of the internal state of a 2D granular slope driven towards its stability limit, θ_A. They related precursors of avalanches to the intermittent mobilization of friction forces between the grains along some long-range correlations of the structure.

B. Humidity effect

In order to integrate the humidity effect in our experimental investigation, we are, firstly, collecting information through previous similar studies. For example, Gómez-Arriaran et al. [20] studied the evolution of maximum stability angles θ_A and repose angles θ_R of tilted granular pile with glass grains of size $0.5mm$, $1mm$ and $2mm$ under controlled relative humidity Φ between $5\,\%$ and $97\,\%$. They observed that these angles are invariant in pendular state ($\Phi < 50\,\%$) and increase with relative humidity in funicular and capillary state. The most important result shown in this study is that the maximum stability angle is higher in capillary state for small grain diameter, and can reach $90°$. These results confirm that the cohesion between grain is better when the grains are small [21]. Lets go in more details.

Some authors [22, 23] have studied the relationship between cohesion and the adhesion forces between grains in a pile when a meniscus is created between grains. These studies have established that the maximum angle of stability θ_A varies exponentially with the initial time before the experiments. Unfortunately they were performing experiments only up to $\Phi = 45\,\%$ which is far from the range over which the influence on the stability and cohesion of the granular medium is expected to be important. Other authors [24, 25] noted that the depth of the avalanche plane and the angle of repose positively correlate with the moisture content up to a maximum saturation value, which depends on the grain size only. Fraysse et al. [26] have carefully controlled Φ by injecting water vapor in a rotating drum that contained the granular medium. Thus, the control parameter to quantify the moisture content was the relative vapor pressure (P_v/P_{sat}, where P_v: vapor pressure and P_{sat}: saturated pressure), i.e., the relative humidity. They stated that the angle of repose θ_R slightly decreased and the angle of maximum stability θ_A increased when the moisture content was increasing.

In Mason et al. [27], a method of tilting a wet granular packing was used to determine the relationship between the angle of maximum stability θ_A and moisture, which is referred here to the volume fraction of liquid. Other authors [1, 3] also identified a relationship between the relative humidity and the characteristic angles of an inclining box filled with $2mm$ diameter glass beads.

One of the key question of these methods is that the water is not necessarily homogeneously distributed and it was difficult to check this fact. Indeed, the rigorous control of Φ and hygroscopic equilibrium time is necessary to avoid this inhomogeneity and achieve a

uniform distribution of the moisture content in the granular medium at a given hygroscopic and cohesive state. We will see this problem later on in this article.

The main difference between a dry and a wet granular medium lies in the cohesive force between grains generated by moisture. The cohesion between two spheres [28], i.e., the attraction force between two spheres due to a liquid bridge between them, is linked to the surface tension which is the cause of the capillary pressure in the neck of the bridge. Rumpf [29] proposed a model for determining the cohesion tension in a granular medium of identical spherical grains from the force of cohesion per liquid bridge. Crassous et al. [21] have shown the evolution of the adhesive force between two grains versus distance at a given humidity rate through atomic force setup measurements.

In the continuum approach, the Mohr-Coulomb criterion describes the avalanche phenomenon in terms of shear stress (τ) and normal stress (σ) modified by the capillary condensation, which creates additional cohesion between grains, resulting in a "normal cohesive stress" in the medium (σ_c) and in a new total normal stress. This cohesive stress leads to increments in the angle of maximum stability θ_A for a wet granular packing. Indeed, as the height of the packing $'H$ increases, the normal stress corresponding to the weight of the pile also increases ($\rho g H$), but the cohesive forces remain constant irrespective of the size of the pile. As confirmed in Gómez-Arriaran et al. [20], if the packing depth does not influence the cohesion, failure has to occur at the base of this packing (controlled by the Mohr-Coulomb criteria) and the position will depend on the cohesion degree. In some cases, the cohesion provided by liquid bridges in the capillary cohesive state is sufficiently strong to ensure that the grains remain up to a high possible angle ($\theta_A \approx 90°$) So, when the granular medium is in funicular and pendular cohesive states, the granular medium is more appropriately considered as discrete. In this condition, all surface grains attain new stable positions which implies that the avalanche affects mainly the grains at the free surface of the packing.

In both models, continuum and discrete, we can conclude that the cohesive effect of liquid bridges increases the stability of the granular packing: The continuum model predicts that the failure avalanche plan is at the bottom of the packing, and the angle of maximum stability will depend on the size of the packing. For the discrete model, the noticeable part of the failure occurs at the surface and the maximum stability angle is independent of the size of the pile. Our results in section V will confirm these two possibilities according to the different experimental conditions. Recent researches demonstrate the linear dependency

between the angle of maximum stability and the time of exposition to ambient relative humidity before the avalanche [30].

III. PACKING PREPARATION AND TILTING PROCESS

To accomplish the goals of this study, an experimental setup was mounted allowing (1) the detection of the grains rearrangements at the free surface of granular pile, (2) the detection of surface angle of granular pile and (3) the control of relative humidity. The experiments consist in slowly and continuously inclining a box containing grains and following the dynamics of wet granular pile during the inclination. Tested granular piles at high humidity rates were previously conditioned during time between three weeks down to two days to desired relative humidity conditions in order to observe the possible hygroscopic equilibrium through all the pile.

A. Geometrical piling

Our initial goal is the generation of dense homogeneous packings of spheres in a reproducible manner. This is crucial for having the possibility of comparing results coming from different experimental conditions. We have achieved this goal by using the so-called same "history" of the packing fabrication [31].

We are using a Plexiglas box with $6.5\,cm$ width, $11\,cm$ length and $6\,cm$ height. A grid with a mesh size twice larger then the bead diameter is initially placed at the bottom of the box. Then we fill the box with grains up to the desired height (between $2\,cm$ up to $6\,cm$). We check horizontally the packing box in order to create a quasi flat surface. Then we pull out vertically the grid to generate an homogeneous dilute packing structure. When the required height is chosen as a full fill box solution, we pass a metallic bar to eliminate all the grains sitting at a position higher than the box height. When high humidity conditions are needed, all boxes were made in the same protocol then conditioned to the desired relative humidity for a given number of days in order to ensure that the liquid bridges are formed through all the granular pile (see III B). Then we place this box on top of a rotating tray. The rotation of this tray is controlled by an electrical linear actuator (Fig. 1). The inclining velocity is selected about $0.08^\circ/s$. It is chosen after verifying that the inclination is carried out in

quasi-static regime which is confirmed by the very small Froude number $Fr = 1.05\,10^{-4}$. . Then we began to incline the box from the horizontal position up to the maximal available angle of the setup (i.e. 75°) which can produce successive precursors or/and avalanches.

We performed our experiments by using glass grains with $0.2mm$, $0.5mm$ and $0.75mm$ diameters, and polystyrene grains with $0.15mm$ diameters.

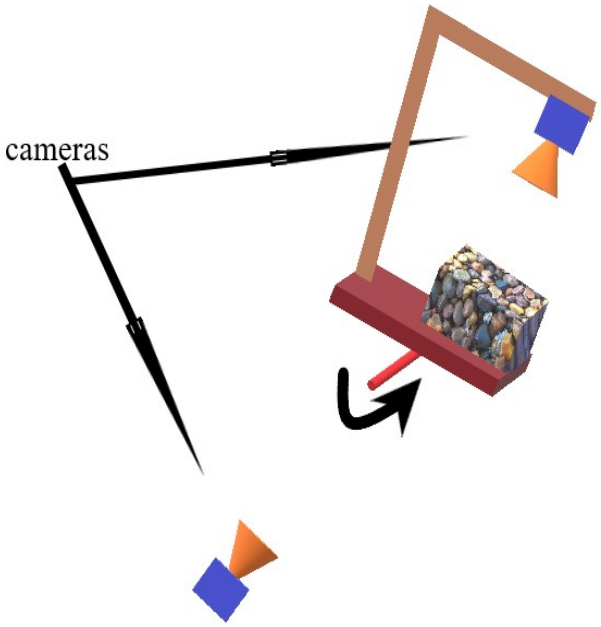

FIG. 1: Schematic view of the setup. A horizontal linear actuator is linked to a vertical bar glued to the rotating plane in order to assure the right rotation rate. A camera shooting the top surface of the packing is maintained with a L-shape bar and rotates with the rotating plane. Another camera is placed horizontally at $1\,m$ away from the moving system to record the full lateral view of the setup.

B. Humidity control

As it was too complicate to manage a large box which can contains the packing box, the tilting setup, the horizontal camera and the vertical camera on the L-shape bar, we have decided to use the ambient conditions for low humidity rates (up to 70%) and to manage an humidity control chamber close to the experimental setup for higher values.

This chamber is made on Plexiglas with width = $36\,cm$, length = $68\,cm$ and an height = $36\,cm$. This solution can allow to store in the same condition up to ten packing boxes containing different experimental grain compositions (bead size or material, filling rate, and so on...). On the bottom of this container box is positioned a large flat plate on which is placed a saturated salt solution mixed with pure water on excess. In this manner, we can control the relative humidity in this chamber by using adequate salts solutions with distilled water (RH for $NaCl$: $\approx 75\,\%$, KCl: $\approx 84\,\%$, KNO_3: $\approx 94\,\%$). The relative humidity and the temperature inside the chambers were recorded every 5 min by two USB sensors. After the chosen "conditioning" time, we can take one box ata time and place it on the rotating tray for doing our experiment. The duration of the transfer and also the full tilting experiment remains quite small (less than 10 minutes), and taking in count the low velocity of the vapor diffusion process through the grain interstitials, we can assume that the quality of the cohesive contact in the free surface of the packing (mainly the top one) is not altered.

IV. OPTICAL TECHNIQUES MEASUREMENTS

In order to fully catch the grain displacement events, we used two cameras to film the experiment: one mounted above the free surface of the granular pile and which rotates with the tray through a L-shape bar and the other one which is placed on a tripod one meter away from the lateral side (Fig. 1). These two optical measurements are captured quasi-simultaneously and both sets of images are processed by ImageJ software. In this example, the box is tilted **continuously** at a rate of $0.08°/s$

Surface angles of the granular pile are measured through the lateral video recording. Those images are registered at a frequency of 30 frames per second and a resolution of 640 by 480 pixels. The video record starts not perfectly synchronized with the surface acquisition process but it will be possible to do it after (see below). As visible in Fig. 2(a), the surface of the packing is easily detectable as having a higher grey level all along a fine visible thick line. After thresholding this line, a simple measurement of the mean angle of the XY pixel line can give us the surface angle. By default, due to the packing construction, this surface angle is exactly the tray angle during the initiation of the movement of the experiment (i.e. at least, xup to the first event: precursor or avalanche). This can allow us to determine the rotation speed (slope and origin of the line) which can define the tray rotation angle

during all the experiment. Figure 2(b) shows the evolution of the surface angle obtained for a packing with a $5\,cm$ height, bead diameter of $0.2\,mm$ humidity rate of $43\,\%$ for a temperature of "26°. The different ratchets observed here are successive reorganization of the surface before grains went outside the packing box.

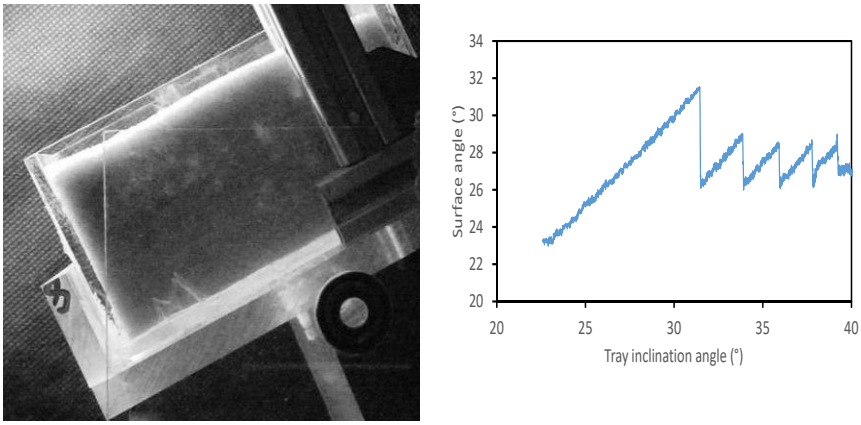

(a) (b)

FIG. 2: Lateral view and its evolution versus the tilting tray rotation for a packing with a $5\,cm$ height, bead diameter of $0.2\,mm$ humidity rate of $43\,\%$ for a temperature of "26°.

Grains rearrangements that are observed on the free surface of granular pile are recorded through the upper side every $0.45\,s$ following the method described previously [4, 6, 12]. Images processing are based on the subtraction of two successive images thresholded higher than the image noise acquisition and produce the pixel map of moved spheres on the surface. These pixels are, by default, a direct link to at least one sphere move and can allow us to define the surface S of rearranged grains. Then this moved grains surface S is normalized by the total surface of the observation zone S_0 and plotted as a function of tilting angle (Fig. 3).

In our experiment, the largest events can represent precursors of avalanche or one of the successive avalanches. The first avalanche transition can be obtained by combining and synchronizing the two views. In Fig. 4, the two optical measurements are then plotted at the same tray inclination angle and we can easily identify avalanche events from precursor ones.

So this full optical technique analysis can allow us to extract all the possible information concerning one experiment: precursor and avalanche position, interval inclination angle

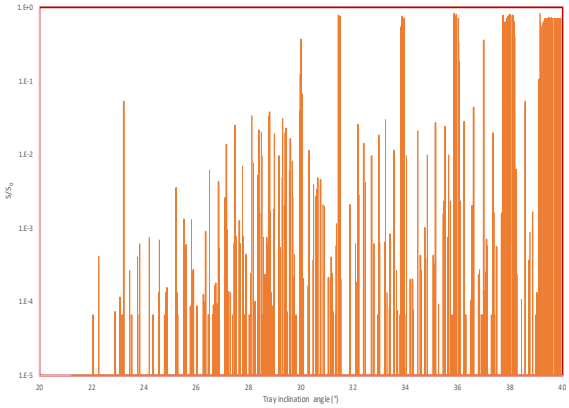

FIG. 3: Evolution of the surface fraction. The relative surface ratio is plotted in a logarithm scale inorder to see the precursor amplitude evolution described by Nerone et al. [4].

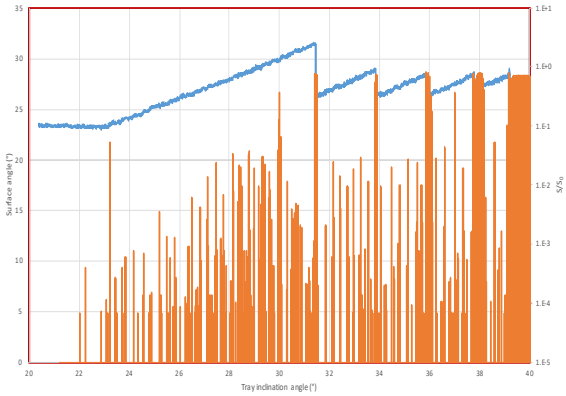

FIG. 4: Evolution of the two views with synchronization.

between precursors before the first avalanche, existence or not of precursors during the following avalanches, and so on.... The two next sections will show all the comparison results; the section V will concern only glass beads of '500 μm and the two following ones (section VI and VII) all the other conditions.

V. ANALYSIS OF THE RESULTS FOR $500\,\mu m$ GLASS BEADS

Several physical parameters can control our experiments such as filling height, humidity rates and conditioning times, bead sizes, bead properties, ...In the following subsections V A and V B, we will look at the effect of the filling heights and the variation of the humidity rates on the precursor and avalanche behaviours for monosize glass beads of $500\,\mu m$ diameter only. So we will start by the filling rate.

A. Filling height effect

By opposition of the rotating drum studies, where no lower bottom wall can limit the initiation of the avalanche (i.e. only the local instability of the pile can generate the beginning of the flow), the tilting box studies, by construction, imply that a bottom wall can avoid some grain movements due to its long term geometrical influence.

1. Avalanche Analysis

According to Gómez-Arriaran et al.'s results [20], we can also observe that the successive avalanche angles decrease after the first one and finally reach a plateau (Fig. 5). And, in the same figure, by comparison with Aguirre et al.'s observation [3], we can see the influence of the bottom wall through its number of layers order propagation. The behaviour is quite different for a filling height of $2\,cm$ which corresponds to around 40 layers from higher values such as 3 or $4\,cm$ (i.e. 60 or 80 layers). This behaviour is quite far from the Aguirre's experiments [1] which located the transition around 16 layers only. This difference is due to our filling process which implies a more homogeneous packing structure but with a smaller packing fraction due to the pulling out of the grid (comparison with Fig.5 in [3]). If we take into account the information from the Fig. 5 on the effective height effect on our experiments,we will focue our results for a filling rate higher than $2\,cm$.

In this case, we can observe that the avalanche angle θ_A is increasing with the filling rate and the repose angle θ_R is also mainly decreasing with height, except for $H = 2\,cm$ where the bottom filling organisation can affect the local displacement of the beads. This first behaviour can be easily interpreted along the number of layers structural effect: higher number of layers means higher packing fraction due to the increase of the amount of material

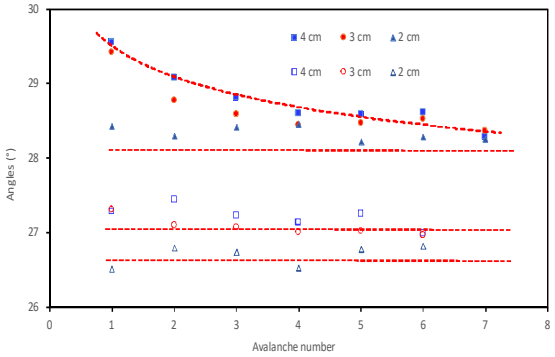

FIG. 5: Influence of the filling rates on the successive avalanche behaviour. Each point is a mean average of more than ten individual runs made inside a relative humidity environment equal to $54\,\%RH$. For height equal to $2\,cm$ (≈ 40 layers) the avalanche and the repose angles are constant. For higher values (> 40 layers) we can recover the behavior visible in [20].

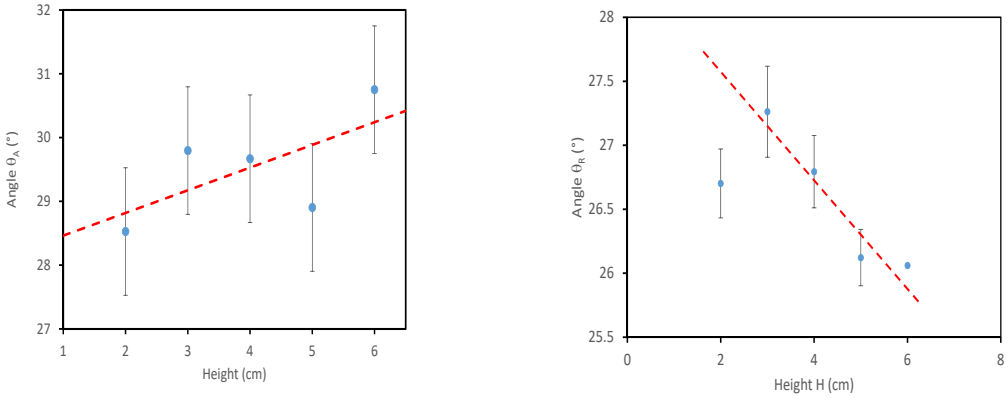

(a) (b)

FIG. 6: Evolution of the maximal stability θ_A and the repose θ_R angles for the different available filling heights. Each point is a mean average of all available data collected for all the available experiments made with an humidity rate lower than $70\,\%$ (reason is seen in Fig. 9(a)).

along the height (classically named as ρgH). This fact allows less possibility of shearing ofr

the lower layers.

Even if the angles θ_A is increasing and θ_R is decreasing with the filling heights, we can observe that the difference remains quite constant (Fig. 7). This observation will allow us to assume that, except for the smaller height of $2\,cm$, we can use all the results obtained with different filling levels for the global analysis of the other parameter evolution.

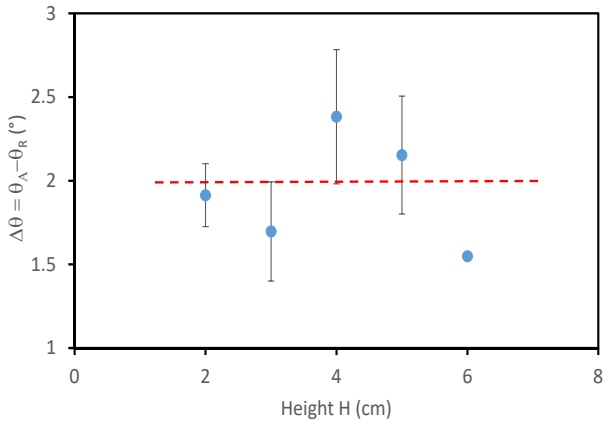

FIG. 7: Evolution of the angle difference between θ_A and θ_R versus the filling height H for experimental conditions identical at the Fig. 6.

2. Precursors Analysis

As already mentioned, the appearance of the first precursors and also the difference angle between two successive precursors is crucial to understand the structural internal interaction and to predict the following avalanche event. We can see these two informations in Fig. 8

We can see that higher the filling rate, higher the angle for the appearance of the first precursor and also the inter-precursor angle. These results can be explained in the same context of the previous observation for θ_A and θ_R: higher packing fraction for higher number of layers so less possibilities of shearing. According to these series of results, we can manage the analysis of the results for different humidities rates with the height dependency or not. Indeed this possibility can allow us to improve the different statistical behavior analysis.

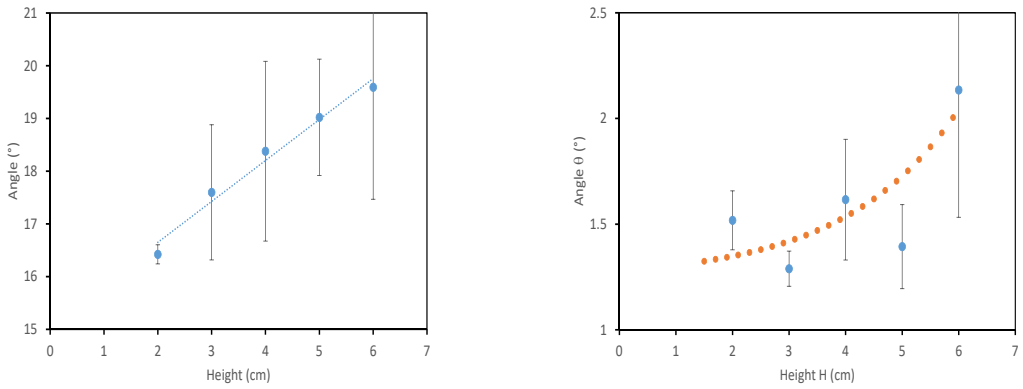

(a) (b)

FIG. 8: Evolution of the appearance angle of the first precursor versus the filling height H (a). Evolution of the inter-precursor angle versus the filling height H (b). Experimental conditions are identical at the Fig. 6.

B. Humidity rate (RH) effect

These experiments are performed in two different humidity conditioning behaviors depending of the range of humidities available naturally (up to 71 %) or the range of chosen ones (in our experimental cases: higher than 70 %). The change of these conditions implies automatically a change in the process before the real tilting experiments. Indeed, in the natural case, we can assume that all the beads are naturally immersed inside the ambient humidity rate. So we don't need to maintain these build packings immobile inside a chamber before doing the experiments. By opposition, when the needed humidity rate is quite high, only samples placed inside a confined chamber saturated at the desired humidity rate during a given time can be used. In this second case, the creation of the capillary bridges inside the porous structure is, by consequence, time dependent (diffusion process inside the porous structure: see section VII).

1. Avalanche Analysis

Our first goal in this part is to reproduce as close as possible the behaviour observed by Gómez-Arriaran et al. [20]. We are using the same kinds of beads (500 μm) and also the

same box dimensions (see in III) but our tilting process is quite different as it is continuous, even after the first avalanche event, at a given inclination rate by opposition of a very slow manual tilting one. The main difference is the possibility for the wet contacts to maintain a longer and stronger contact in the their set of experiments and also the ability to wait some time after a given avalanche event before performing again the tilting process. In our case, we have try to use the smallest available titling rate in order to be close as possible to Gómez-Arriaran's experiments. Figure 9 shows that the evolution of the angles(θ_A and θ_R) follow the behavior of the Gómez-Arriaran's ones [20] except for the order of magnitude. All our results are quite smaller than their results. This fact can be easily explained by the continuous tilting which can generate higher vibrations inside the grain structure. These vibrations can more easily break some internal wet contacts and enhance the fracture propagation in our packings.

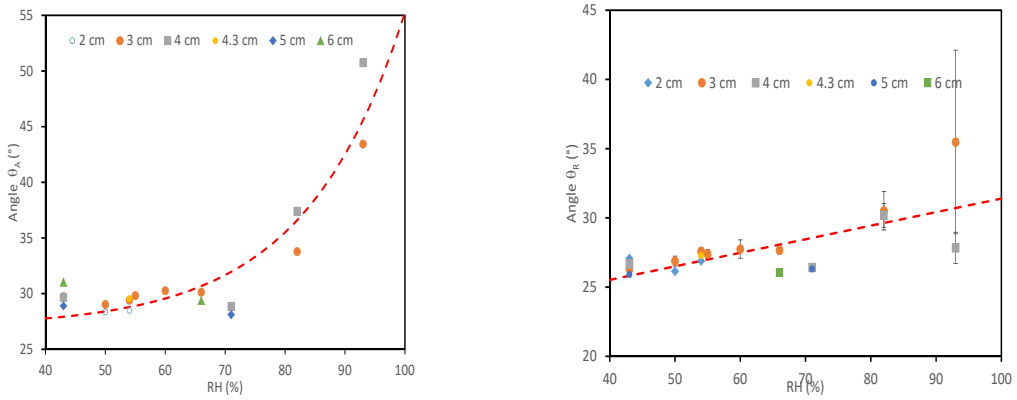

(a) (b)

FIG. 9: Evolution of the avalanche θ_A and the repose θ_R angles versus the humidity rate for the different available filling heights. The results are shown separately for each set of height H. The dashed lines are only guided lines for a better observation. For (a) it is an exponential form.

More generally, we can see that the avalanche angle θ_A is increasing significantly with the humidity rate as described in previous studies [20]. By opposition, the repose angle θ_R remains almost constant for the full range but we have drawn an inclined line line as we can assume that the underling global network of wet contacts can play a role during the landing of the falling beads, fact which will be confirmed in the following section. The difference of

behaviours between the two angles can be also seen in Fig. 10 which represents the difference between the avalanche angle θ_A and the repose angle θ_R for all the filling height range H.

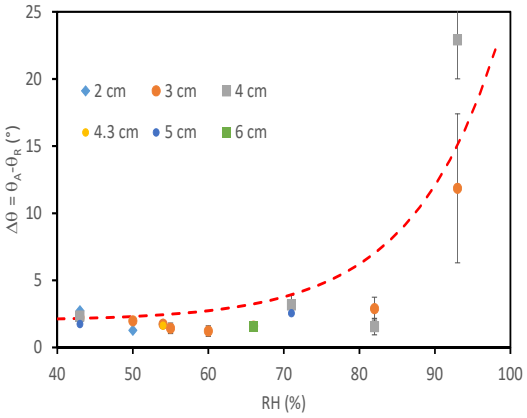

FIG. 10: Evolution of the difference between the avalanche angle θ_A and the repose angle θ_R versus the humidity rate RH for all available filling heights H.

2. *Precursors Analysis*

As observed for the filling height effect, we can look at the influence of the humidity rate on the first appearance of the precursor and also at mean angle difference between these precursors which are present before the first avalanche (Fig. 11).

We have plotted the values forall the available filling heights used in our experiments ($H = 2$ to $6\,cm$) in order to have enough statistical observations. We can see a linear increase of the first precursor appearance with the humidity rates which can be explained by the effect of the increase of the local adhesion force between grains visible on the surface by the possible reorganization shown by the precursor events. By contrast, we cannot observe a clear evolution of the inter-precursor angle value which can be explained as a phenomenon more control by the geometrical organisation of the grain than the adhesion force difference with the humidity rates..

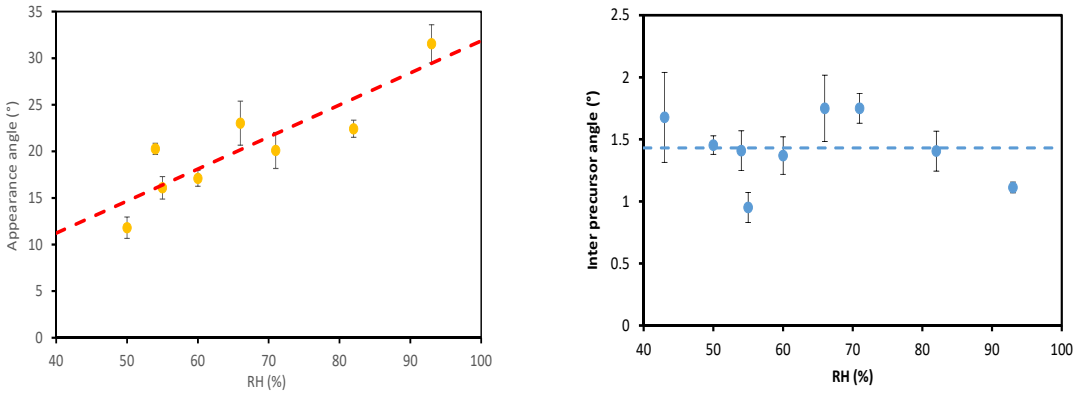

(a) (b)

FIG. 11: Evolution of the appearance angle for the first precursor versus the humidity rate RH (a). Evolution of the inter-precursor angle versus the humidity rate RH (b).

VI. EFFECT OF THE BEAD SIZES AND COMPOSITION

Up to now, we have only described results obtained with beads of diameter 500 μm which were the smallest size used by Gómez-Arriaran [20] to see the humidity influence. So to increase our range of observations; we have performed also experiments under the same mechanical and humidity conditions with glass beads of diameters 200 μm and 750 μm and polystyrene beads of diameter 140 μm. Firstly, we have measured for two new sets of beads the adsorption isotherms in order to observe the evolution of the water content (Fig. 12).

We can see the large increase of the water content for both beads sizes around 70 % which confirms previous results (Fig. 9). So, before this value, no big change for individual contact, or adhesion force, is possible

A. 200 μm glass beads analysis

Firstly, for the 200 μm glass beads, we want to recover the different evolutions observed for the 500 μm glass beads such as the angles of avalanche θ_a and repose θ_R versus the number of avalanches then these angles versus the humidity rate and finally the first precursor appearance. For these studies, we have only performed experiments with packings which fully filled the box ($H = 6\,cm$). Indeed this filling rate was seen before in this paper as the

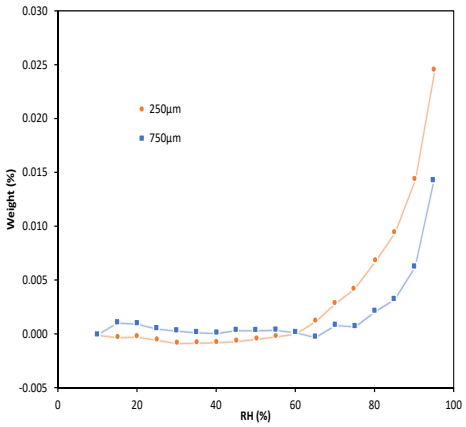

FIG. 12: Influence of the humidity rates on the adsorption isotherms for the two other beads diameters used in this study: $200\,\mu m$ and $750\,\mu m$.

most easy to manage.

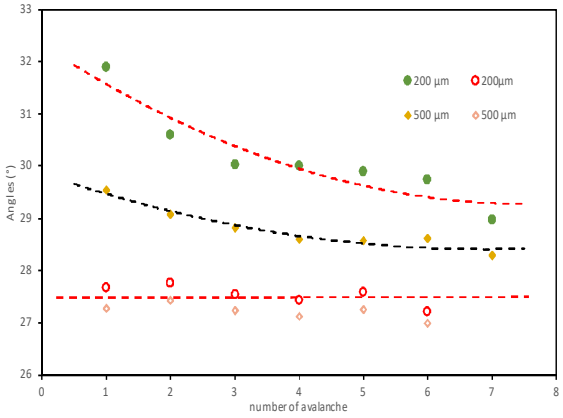

FIG. 13: Evolution of the successive avalanche behaviours for glass beads of $200\,\mu m$ (RH between 43 % and 58 %) and $500\,\mu m$ (HR between 43 % and 66 %). We can recover the classical behaviour already seen before (Fig. 5) and visible in [20]. Each point is a mean vlaue for at least 5 different runs

Figure 13 shows the same behaviour as the one described in Fig. 5 and in the paper of Gómez-Arriaran [20]. We can notify that the angle of repose θ_R is quite similar for both

diameter sizes which tends to demonstrate that the roughness of the surface structure is not playing a crucial role. Indeed, in our case $\theta_R(200\mu m)$ is equal to $\theta_R(500\mu m)$ for all the diameter and humidity rates available.

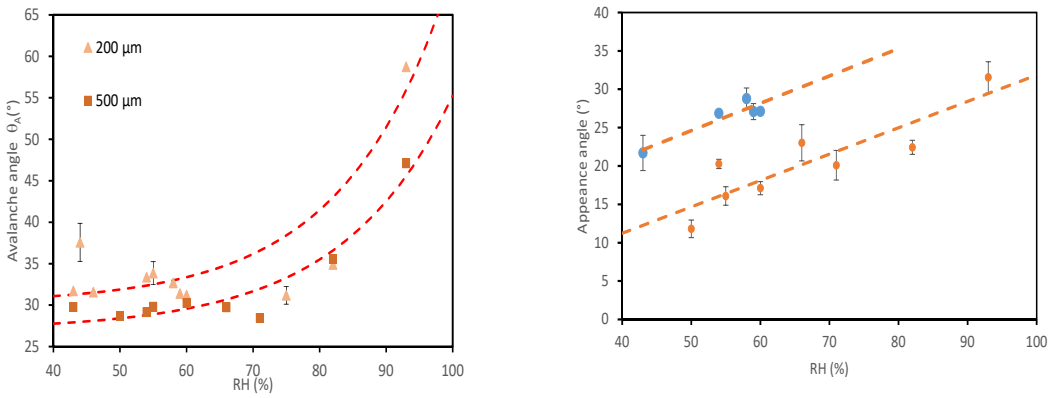

(a) (b)

FIG. 14: (a) Evolution of the avalanche angle θ_A versus the humidity rate for a filling height $H = 6\,cm$ for glass beads of $200\,\mu m$ and $500\,\mu m$. (b) Evolution of the first precursor angle versus the humidity rate for a filling height $H = 6\,cm$ for glass beads of $200\,\mu m$ and $500\,\mu m$.

Figure 14 shows that even if the evolution of the two classical angles of avalanches θ_A and repose θ_R are almost invariant within this range of humidity rates. The appearance angle of the first precursor is increasing with the humidity rates which confirms that this evolution is similar to the one observed for the beads of $500\,\mu m$ (fig. 11).

B. 750 μm beads analysis

Secondly, we have extended our studies to the $750\,\mu m$ glass beads such as the angles of avalanche θ_a versus the humidity rate and finally the first precursor appearance and the inter-precursor intervals. For these studies, we have also only observed experiments with packings which fully filled the box ($H = 6\,cm$). Figure 15 shows that the avalanche angle is independent of the humidity rate which is quite different to the results of Gómez-Arriaran [20]. The difference of behaviour is still explained by the 'large' velocity' used in our automatic setup compared to the slow manual motion used by them.

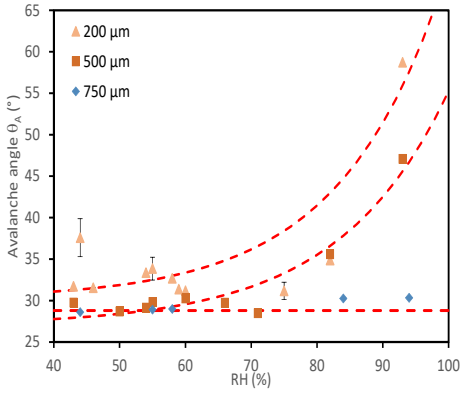

FIG. 15: (a)Evolution of the avalanche angles θ_A versus the humidity rate for a filling height $H = 6\,cm$ for glass beads of $200\,\mu m$, $500\,\mu m$ and $750\,\mu m$.The dash lines correspond to the two fits shown in Fig. 9 for 200 and $500\,\mu m$ and a simple linear one for $750\,\mu m$

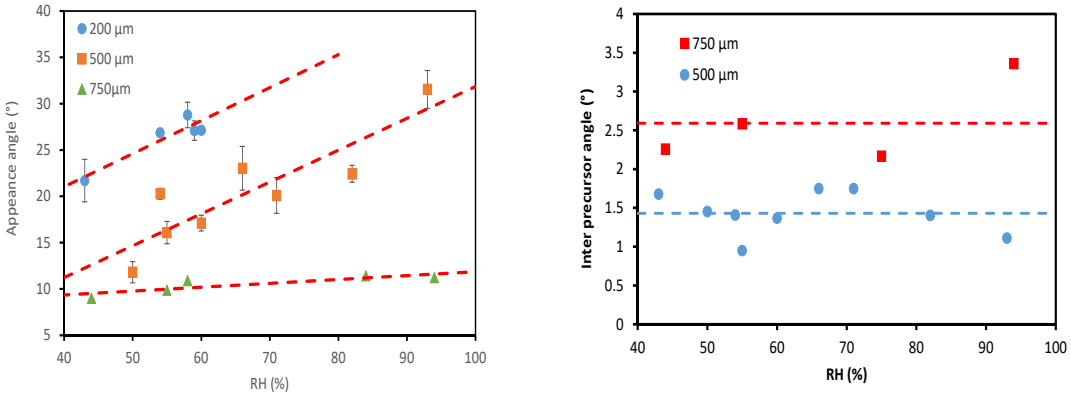

(a) (b)

FIG. 16: (a)Evolution of the first precursor angle versus the humidity rate for a filling height $H = 6\,cm$ for glass beads of $200\,\mu m$, $500\,\mu m$, and $750\,\mu m$. (b) Evolution of the inter precursor angle versus the humidity rate for a filling height $H = 6\,cm$ for glass beads of $200\,\mu m$, $500\,\mu m$, and $750\,\mu m$.

Figure 16 shows that the first precursor appearance is still increasing with the humidity rate but much smaller than the results for smaller glass beads. In the same manner the inter-precursor interval remains constant in both cases but with different amplitudes which

is naturally dependent to the grain size local structure.

C. Polystyrene bead composition analysis

Finally, we have extended our studies to the 140 μm polystyrene beads. These beads have a quite different water contact angle 87.4° and the critical surface tension is 40 $mM.m^{-1}$ (see in https://www.accudynetest.com) compared to 22° and 70 $mM.m^{-1}$ for glass beads respectively

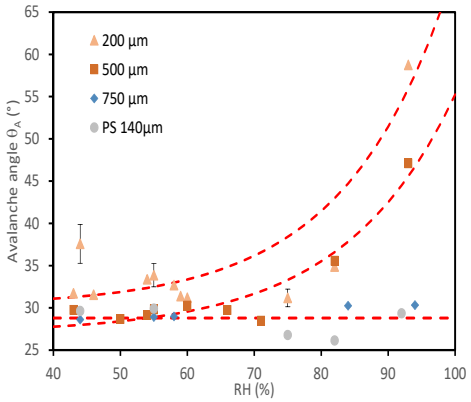

(a) (b)

FIG. 17: Evolution of the avalanche angles θ_A versus the humidity rate for a filling height $H = 6\,cm$ for glass beads of 200 μm, 500 μm and 750 μm and polystyrene beads of 140 μm. The dash lines correspond to the fits shown in Fig. 9 for the glass beads of 200 and 500 μm and a simple horizontal line one for 750 μm and also for the polystyrene beads of 140 μm.

We can see in Fig. 17 that the maximal stability angle of the polystyrene beads is not changing with the evolution of the humidity rate which is consistent with our expectation. Indeed, these beads are hydrophobic which means that the water meniscus at the contact point remains very small whatever the humidity rates are. And, by consequence, no increase of the adhesion forces is present and can be observed in our experiments. The linear horizontal fits for the glass beads 750 μm and polystyrene beads of 140 μm are identical which confirms this fact. Figure 18 shows that the evolution of the first precursor appearance is a combination of the geometrical effect (comparison with the 200 μm glass beads), the non

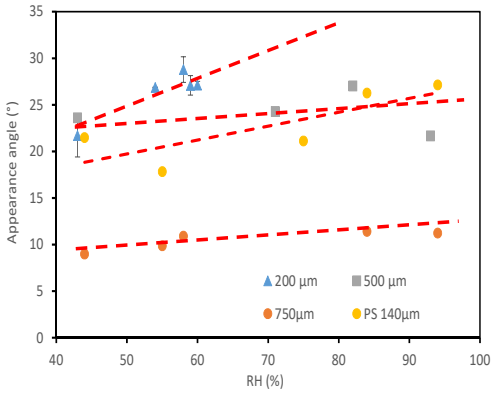

FIG. 18: (a)Evolution of the first precursor angle versus the humidity rate for a filling height $H = 6\,cm$ for glass beads of $200\,\mu m$, $500\,\mu m$, and $750\,\mu m$ and polystyrene beads of $140\,\mu m$..

wetting contact effect (comparison with the $750\,\mu m$ glass beads) and finally the different friction coefficient of the material. These fact place the curve between the two other ones.

VII. EFFECT OF THE DURATION OF HUMIDITY SUBMISSION

Finally, we are dealing with a crucial parameter for our studies of the humidity effects: the quality of the humidity distribution inside the full packing. Indeed, as we are dealing with relative small beads (140 to $750\,\mu m$) the permeability of these packings are quite small which can slow down the water vapor diffusion through our static packings. As already well-known for sphere packings [32], the permeability can be evaluated on the basis of the porosity, tortuosity factor and mean pore size () so it scales with the square of the mean pore size, which scales with the sphere diameter. When we have deal with natural humidity rate (i.e. up to 71% in our case), so we can assume that the water is surrounding uniformly every beads, we can pack the beads pilings and start the experiment right away. By opposition, for higher humidity rates, the packing is done previously and stored inside a given humidity rate environment and two fans are used to ventilate these boxes which necessitate some times to propagate the water vapor content down to the bottom of the packings. Indeed, by construction our packings have only one free accessible upper surface in contact with the humid air. As demonstrated by Gómez-Arriaran et al. [20] this waiting time is crucial

for getting a perfect structure so we are looking at our results following this point view. Figure 19 shows the means values of the full behaviour of three different samples during the avalanche processes submitted to an humidity of 94 % during either one week of or only two days.

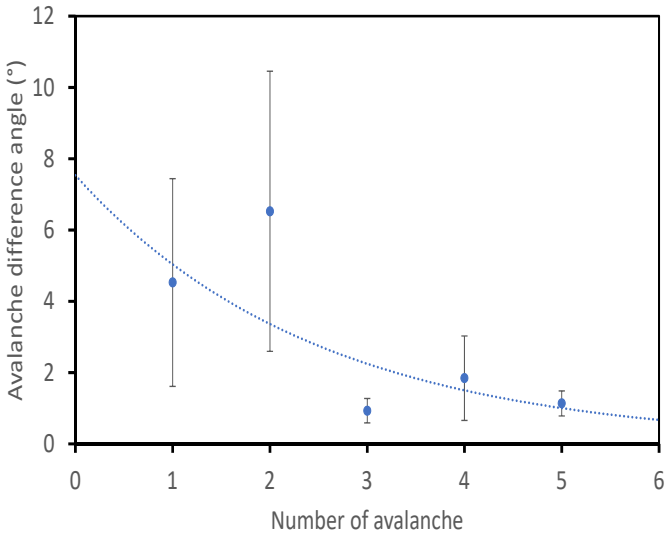

FIG. 19: Difference between the avalanche angles for two sets of packings submitted to the same humidity rate (93 %) but during two different durations (one week versus two days).

We can see a significant difference between these two behaviours which confirms that two days is largely not enough to generate an homogeneous cohesive packing. In complement, we can also mention that one week is still too small especially for small beads packings (i.e. low permeability) and high humidity rate such in this case. So we have also perform two sets of experiments in which the packings were immersed during four weeks or one week at an humidity rate of 82 %. In this case we have observed a relative diminution of the avalanche of angle of 17 % to be compared to the 10 % observed in the Fig. 19.

VIII. CONCLUSION

So in conclusion, we have presented here a study to characterize the influence of the humidity rates on the rearrangement events inside sphere packing when it is inclined up to

a granular avalanche.

Studies reported before have shown the existence of surface rearrangements of grains before an avalanche: small (few individual grains in movement) and large rearrangements or precursors (number of displaced grains of the order of one or more packing layers). We have shown here that these precursors (first appearance and periodicities) are depending to the grain size, grain properties and also, of course, to the inner humidity rates.

IX. ACKNOWLEDGMENTS

This work was partially done during the LIA PMF and the ECOS-SUD E15A043 programs. A grant for external exchange of PhD student was also obtained by C. el Tannoury in order to perform experiments during two months in GMP-UBA. IGA thanks XXX Departamento de Educación del Gobierno Vasco y al grupo ENEDI de la UPV-EHU.

---

[1] M.A. Aguirre, N. Nerone, A. Calvo, I. Ippolito, and D. Bideau. Influence of the number of layers in the equilibrium of a granular surface. *Physical Review E*, 62(1):738–743, 2000.

[2] N. Nerone, M.A. Aguirre, A. Calvo, I. Ippolito, and D. Bideau. Surface fluctuation in a slowly driven granular system. *Physica A*, 283:218–222, 2000.

[3] M.A. Aguirre, N. Nerone, A. Calvo, I. Ippolito, and D. Bideau. Granular packing: influence of different parameters on its stability. *Granular Matter*, 3:75–77, 2001.

[4] N. Nerone, M.A. Aguirre, A. Calvo, D. Bideau, and I. Ippolito. Instabilities in slowly driven granular packing. *Phys. Rev. E*, 67:011302, 2003.

[5] E. Charlaix and M. Ciccotti. chap. 12 capillary condensation in confined media. In K. D. Sattler, editor, *Handbook of Nanophysics: Principles and Methods*. CRC Press, Boca Raton, FL, 2010.

[6] S. Kiesgen de Richter, G Le Caër, and R. Delannay. Dynamics of rearrangements during inclination of granular packings: the avalanche precursor regime. *J. Stat. Mech.*, page 04013, 2012.

[7] P. Boltenhagen. Boundary effects on the maximal angle of stability of a granular packing. *The European Physical Journal B*, 12(1):75–78, oct 1999.

[8] P. Evesque, D. Fargeix, P. Habib, M. P. Luong, and P. Porion. Gravity and density dependences of sand avalanches. *J. Phys. I France*, 2:1271, 1992.

[9] A. Jarray, V. Magnanimo, and S. Luding. Wet granular flow control through liquid induced cohesion. *Powder Technology*, feb 2018.

[10] M. Bretz, J. B. Cunningham, P. L. Kurczynski, and F. Nori. Imaging of avalanches in granular materials. *Physical Review Letters*, 69(16):2431–2434, oct 1992.

[11] M. Duranteau, V. Tournat, V. Zaitsev, R. Delannay, and P. Richard. Identification of avalanche precursors by acoustic probing in the bulk of tilted granular layers. In *Powders and Grains 2013: Proceedings of the 7th International Conference on Micromechanics of Granular Media*, volume 1542, page 650. AIP, 2013.

[12] M. Duranteau, R. Delannay, P. Richard, and V. Tournat. Avalanches and quasi-periodic events in slowly tilted granular media. *Journal of Statistical Mechanics*, 2014.

[13] Y. Zhang and C. S. Campbell. The interface between fluid-like and solid-like behaviour in two-dimensional granular flows. *J. Fluid Mech.*, 237:541, 1992.

[14] R. Fischer, P. Gondret, and M. Rabaud. Transition by intermittency in granular matter: From discontinuous avalanches to continuous flow. *Physical Review Letters*, 103(12):128002, sep 2009.

[15] J. Litster and B. Ennis. *The Science and Engineering of Granulation Processes*. Springer Netherlands, 2004.

[16] N. Nerone and S. Gabbanelli. Surface fluctuations and the inertia effect in sandpiles. *Granular Matter*, 3(1-2):117, jan 2001.

[17] V. Yu. Zaitsev, P. Richard, R. Delannay, V. Tournat, and V. E. Gusev. Pre-avalanche structural rearrangements in the bulk of granular medium: Experimental evidence. *EPL (Europhysics Letters)*, 83(6):64003, sep 2008.

[18] Y. Zhu, C. el Tannoury, R. Delannay, L. Oger, and Y. Le Gonidec. Precursors periodicity during cycling of oscillated sphere packings. *J. Phys. D: Appl. Phys.*, page preprint, 2018.

[19] L. Staron, F. Radjai, and J.P. Vilotte. Granular micro-structure and avalanche precursors. *Journal of Statistical Mechanics: Theory and Experiment*, 2006(07):P07014–P07014, jul 2006.

[20] I. Gómez-Arriaran, I. Ippolito, R. Chertcoff, M. Odriozola-Maritorena, and R. De Schant. Characterization of wet granular avalanches in controlled relative humidity conditions. *Powder Technology*, 279:24–32, jul 2015.

[21] J. Crassous, M. Ciccotti, and E. Charlaix. Capillary force between wetted nanometric contacts and its application to atomic force microscopy. *Langmuir*, 27:3468–3473, 2011.

[22] F. Restagno, L. Bocquet, and E. Charlaix. Where does a cohesive granular heap break? *The European Physical Journal E*, 14(2):177–183, jun 2004.

[23] L. Bocquet, E. Charlaix, S. Ciliberto, and J. Crassous. Moisture-induced ageing in granular media and the kinetics of capillary condensation. *Nature*, 396(6713):735–737, dec 1998.

[24] A. Samadani and A. Kudrolli. Angle of repose and segregation in cohesive granular matter. *Physical Review E*, 64(5):051301, oct 2001.

[25] S. Nowak, A. Samadani, and A. Kudrolli. Maximum angle of stability of a wet granular pile. *Nature Physics*, 1(1):50–52, oct 2005.

[26] N. Fraysse, H. Thomé, and L. Petit. Humidity effect on the stability of a sandpile. *The European Physical Journal B*, 11(4):615–619, oct 1999.

[27] T. G. Mason, A. J. Levine, D. Ertaş, and T. C. Halsey. Critical angle of wet sandpiles. *Physical Review E*, 60(5):5, nov 1999.

[28] C. D.Willett, M. J. Adams, S. A. Johnson, and J.P.K. Seville. Capillary bridges between two spherical bodies. *Langmuir*, 16(24):9396–9405, nov 2000.

[29] H. Rumpf. *The strength of granules and agglomerates*, pages 379–418. Interscience Publishers, New York, 1962.

[30] I. Gómez-Arriaran, I. Ippolito, R. Chertcoff, M. Odriozola-Maritorena, and R. De Schant. *submitted*, 2018.

[31] D. Bideau, E. Guyon, and L. Oger. Granular media: Effects of disorder. In J. C. Charmet, S. Roux, and E. Guyon, editors, *Disorder and Fracture*. Springer US, 1990.

[32] E. Guyon, L. Oger, and T.J. PLona. Transport properties in sintered porous media composed of two particle sizes. *Journal of Physics D: Applied Physics*, 20(12):1637–1644, dec 1987.